Inorganic Chemistry

Article

pubs.acs.org/IC

$Bi_3Cr_{2.91}O_{11}$: A Ferromagnetic Insulator from Cr^{4+}/Cr^{5+} Mixing

Wei Yi,[†] Yoshitaka Matsushita,[‡] Akira Sato,[‡] Kosuke Kosuda,[‡] Michiko Yoshitake,[§] and Alexei A. Belik*,[†]

[†]International Center for Materials Nanoarchitectonics (WPI-MANA), National Institute for Materials Science (NIMS), 1-1 Namiki, Tsukuba, Ibaraki 305-0044, Japan

[‡]Materials Analysis Station, National Institute for Materials Science, 1-2-1 Sengen, Tsukuba, Ibaraki 305-0047, Japan

[§]MANA Nano-Electronics Materials Unit, National Institute for Materials Science (NIMS), 3-13 Sakura, Tsukuba, Ibaraki 305-0003, Japan

Supporting Information

ABSTRACT: The search for materials with ferromagnetic and semiconducting/insulating properties has intensified recently because of their potential use in spintronics. However, the number of materials is rather limited because of conflicting requirements needed for the appearance of ferromagnetic and insulating properties. Here we show that $Bi_3Cr_{2.91}O_{11}$ belongs to the scarce family of ferromagnetic insulators. $Bi_3Cr_{2.91}O_{11}$ was synthesized at high pressure of 6 GPa and high temperature of 1570 K. Its crystal structure and properties were studied using single crystals. It crystallizes in the $KSbO_3$-type structure with space group $Pn\bar{3}$ and the lattice parameter a = 9.2181(2) Å. $Bi_3Cr_{2.91}O_{11}$ has almost a 1:1 mixture of Cr^{4+} and Cr^{5+} ions distributed in one octahedral crystallographic site. $Bi_3Cr_{2.91}O_{11}$ is a rare example of oxides having chromium ions in unusual oxidation states. The presence of Cr^{4+} and Cr^{5+} results in ferromagnetic properties with ferromagnetic Curie temperature T_C = 220 K.

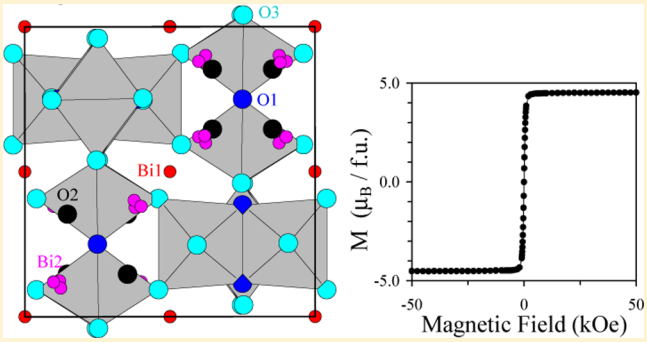

1. INTRODUCTION

The search for materials with ferromagnetic and semiconducting properties has intensified recently because of their potential use in spintronics.[1] However, the number of materials is rather limited because of conflicting requirements in crystal structures, chemical boding, and electronic states needed for the appearance of ferromagnetic and semiconducting properties at the same time.[1,2]

Ferromagnetism is usually associated with metallic conductivity. This tendency is observed not only in simple metals such as Fe (the ferromagnetic Curie temperature (T_C) is 1043 K), Ni (T_C = 627 K), and Co (T_C = 1388 K)[3] but also in oxide ceramics such as CrO_2 (T_C = 386 K),[3] $SrRuO_3$ (T_C = 165 K),[4] $LaMnO_{3+\delta}$ ($\delta \approx 0.14$, $T_C \approx 200$ K),[5,6] $La_{1-x}Sr_xMnO_3$ ($x \approx 0.3$–0.5, $T_C \approx 350$ K),[7] and EuO_{1-x} (T_C = 69 K).[3,8] Insulating/semiconducting ferromagnets are always exceptional cases from the general rule, and they are attractive not only from the practical point of view but also from the viewpoint of understanding the mechanism of ferromagnetism.[1] For example, the discovery of ferromagnetism in diluted semiconductors (e.g., (Ga, Mn)As, TiO_2, and In_2O_3)[9,10] has generated much attention, but the origin of ferromagnetism in those materials is still a matter of debate.

Materials with insulating/semiconducting and true ferromagnetic properties can be exemplified by $BiMnO_3$ (T_C = 100 K),[11,12] $LaMnO_{3+\delta}$ ($\delta \approx 0.10$; $T_C \approx 200$ K),[5,6] $La_{1-x}Sr_xMnO_3$ ($x \approx 0.1$; $T_C \approx 200$ K),[7] $K_2Cr_8O_{16}$ (T_C = 180 K, a semiconductor below 95 K),[13] $CrBr_3$ (T_C = 33 K),[3] and R_2NiMnO_6 (R = La–Lu and Y; T_C = 50 K for Lu, and T_C = 295 K for La).[2,14] We found recently that $Bi_3Mn_3O_{11.6}$ with T_C = 315 K possesses a new record high T_C for this class of materials.[15,16]

In this work, we prepared $Bi_3Cr_{2.91}O_{11}$ using a high-pressure high-temperature method and showed that it is also a ferromagnetic insulator similar to $Bi_3Mn_3O_{11.6}$. $Bi_3Cr_{2.91}O_{11}$ has a rather unusual mixture of Cr^{4+} and Cr^{5+} ions. The presence of almost a 1:1 mixture of Cr^{4+} and Cr^{5+} ions distributed in one crystallographic site results in ferromagnetic properties.

2. EXPERIMENTAL SECTION

Samples in our work were prepared from stoichiometric mixtures of Bi_2O_3 (99.9999%, Rare Metallic Co. Ltd.), CrO_2 (99.9%), and CrO_3 (99%, High Purity Chemicals Ltd.). The starting chemicals were weighed and reground in a glovebox, and the starting mixtures were placed in Au capsules and treated under 6 GPa in a belt-type high-pressure apparatus at 1570 K for 2 h (heating rate to the desired temperature was 10 min). After the heat treatment, the samples were quenched to room temperature (RT), and the pressure was slowly released. The resultant samples were black fragile pellets. Single crystals could be found in some samples. The phase purity and oxygen content of CrO_2 were checked and confirmed (by X-ray powder

Received: April 2, 2014
Published: August 4, 2014

   dx.doi.org/10.1021/ic500773b | Inorg. Chem. 2014, 53, 8362–8366

diffraction (XRPD) and thermogravimetric analysis) before its use. However, because of toxicity of Cr(VI) and hydroscopic nature and low melting point of CrO_3, we could not check its oxygen content and assumed its chemical composition to be CrO_3. We tried to prepare different compositions: $Bi_3Cr_3O_{11\pm\delta}$, $Bi_{3-\delta}Cr_3O_{11-1.5\delta}$, and $Bi_3Cr_{3-\delta}O_{11-1.5\delta}$.

Note that we tried to adjust the oxygen content by $KClO_4$ in stoichiometric mixtures of Bi_2O_3 and CrO_2. However, the appearance of BiOCl impurity was found indicating a reaction between Bi_2O_3 and KCl. Therefore, this way was abandoned.

X-ray powder diffraction data were collected at room temperature on a RIGAKU Ultima III diffractometer using Cu Kα radiation (2θ range of 10−80°, a step width of 0.02°, and a counting time of 2 s/step). Laboratory XRPD data were analyzed by the Rietveld method with RIETAN-2000 software.[17] For impurities, we refined only scale factors and lattice parameters, fixing their structure parameters.

Single-crystal intensity data were collected at 293 K using a Bruker SMART APEX single-crystal diffractometer equipped with a CCD area detector and a graphite monochromator utilizing Mo Kα radiation (λ = 0.710 73 Å). Cell parameters were retrieved using SMART software[18] and refined using SAINT software[19] on all observed reflections. Data reduction was performed with SAINT software, which corrects for Lorentz polarization and decay. Absorption corrections were applied using SADABS.[20] Crystal structures were solved by the direct method with SHELXS-97[21] and subsequently refined against all data in the 2θ ranges by full-matrix least-squares on F^2 using SHELXL-97,[21] working on WinGX suite.[22]

Magnetic susceptibilities, χ = **M**/**H**, were measured on a SQUID magnetometer (Quantum Design, MPMS) between 2 and 350 K in different applied fields under both zero-field-cooled (ZFC) condition and field-cooled (FC; on cooling) condition. Isothermal magnetization measurements were performed between −50 and 50 kOe. Electrical resistivity of single crystals was measured by the conventional four-probe method using a Quantum Design PPMS.

X-ray photoelectron spectroscopy (XPS) measurements were recorded with a PHI Quantum 2000 system using a monochromatic Al Kα radiation and 23.50 eV pass energy. The Al Kα X-ray source was operated at a power of 40 W, and the X-ray spot size was set to be 100 μm in diameter. Dual-beam neutralization was used during data collection. The takeoff angle was set to be 45°. Electron-probe microanalysis (EPMA) was performed using a JEOL JXA-8500F instrument. The surface was polished on a fine (0.3 μm) alumina-coated film before the EPMA measurements; and $Bi_4Ti_3O_{12}$ and Cr_2O_3 were used as standard samples for Bi and Cr, respectively.

3. RESULTS AND DISCUSSION

XRPD patterns of samples with the target compositions of $Bi_3Cr_{3-\delta}O_{11-1.5\delta}$ (δ = 0, 0.1, and 0.2) are shown in Figure 1a. $Bi_3Cr_3O_{11}$ consisted of a $KSbO_3$-type cubic phase and a small amount of an impurity phase. The impurity phase was found to be isostructural with γ-$Bi_4V_2O_{11}$.[23] Therefore, the structure parameters of γ-$Bi_4V_2O_{11}$ were used to describe the impurity with the possible composition of Bi_2CrO_{5+x} (space group *I*4/*mmm*, a = 4.0135(2) Å and a = 15.141(1) Å; with the EPMA measurements, we could find an impurity with the Bi/Cr ratio of 2:1). With the increase of the Cr deficiency in $Bi_3Cr_{3-\delta}O_{11-1.5\delta}$, the amount of Bi_2CrO_{5+x} increased.

XRPD patterns of Bi-deficient samples with the target compositions of $Bi_{3-\delta}Cr_3O_{11-1.5\delta}$ (δ = 0.1, 0.2, and 0.3) are shown in Figure 1b. $Bi_{2.9}Cr_3O_{10.85}$ still contained Bi_2CrO_{5+x} impurity; $Bi_{2.7}Cr_3O_{10.55}$ and $Bi_{2.8}Cr_3O_{10.7}$ were single-phase based on the laboratory XRPD data. $Bi_{2.5}Cr_3O_{10.25}$ and $Bi_{2.6}Cr_3O_{10.4}$ samples already contained a detectable amount of CrO_2 impurity (see the Supporting Information; with the EPMA measurements, we could find an impurity that contained only Cr). $Bi_3Cr_3O_{11\pm\delta}$ samples contained Bi_2CrO_{5+x}, CrO_2, or unidentified impurities.

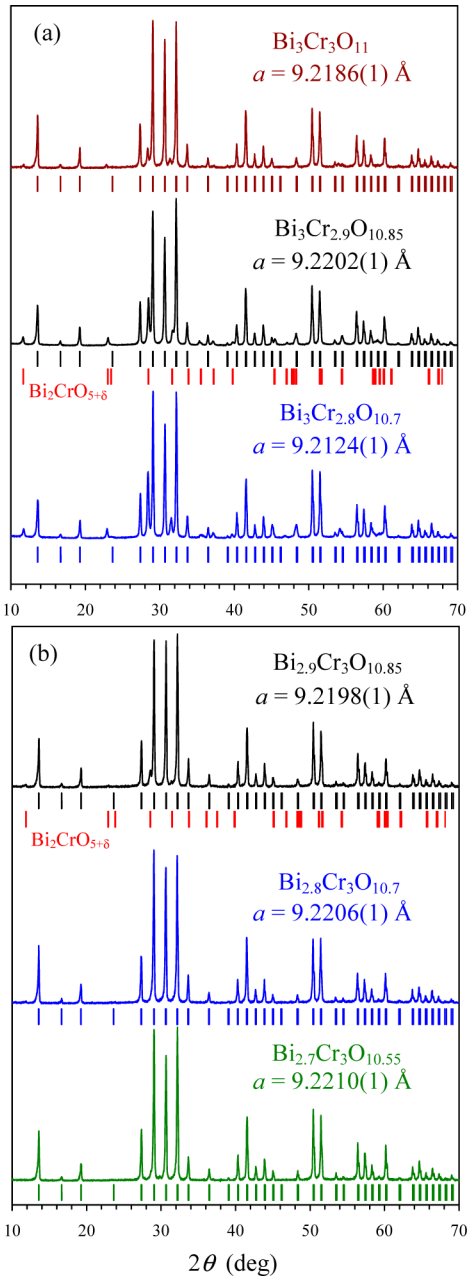

Figure 1. Room-temperature laboratory (Cu Kα) X-ray powder diffraction patterns for (a) $Bi_3Cr_{3-\delta}O_{11-1.5\delta}$ (δ = 0, 0.1, and 0.2) and (b) $Bi_{3-\delta}Cr_3O_{11-1.5\delta}$ (δ = 0.1, 0.2, and 0.3). Bragg reflections are indicated by tick marks for the $KSbO_3$-type cubic phase and $Bi_2CrO_{5+\delta}$ impurity.

The chemical composition of single crystals taken from the samples with the target compositions of $Bi_{2.7}Cr_3O_{10.55}$ and $Bi_{2.8}Cr_3O_{10.7}$ was determined to be $Bi_3Cr_{2.91}O_{11}$ from the single-crystal structural analysis as mentioned below. The discrepancy between the target and single-crystal compositions could originate from the use of CrO_3 (whose composition could deviate from the ideal one) as the starting material or from the presence of amorphous impurity phases undetectable by XRPD. Therefore, single-phase (by XRPD) $Bi_{2.7}Cr_3O_{10.55}$ and $Bi_{2.8}Cr_3O_{10.7}$ samples could be multiple-phase in reality. Therefore, the structure determination and property measurements were performed on selected single crystals. Note that the single-crystal structure analysis is one of the best methods for

dx.doi.org/10.1021/ic500773b | *Inorg. Chem.* 2014, 53, 8362−8366

determination of chemical compositions (under certain conditions that are fulfilled in $Bi_3Cr_{2.91}O_{11}$, such as known chemical elements, a simple crystal structure, large difference in scattering factors, the absence of statistical occupation of one site by different elements, and others).

Crystallographic and refinement results of $Bi_3Cr_{2.91}O_{11}$ from the single-crystal structural analysis are listed in Tables 1 and 2.

Table 1. Crystal Data and Structural Refinement Parameters for $Bi_3Cr_{2.91}O_{11}$.

empirical formula	$Bi_3Cr_{2.91}O_{11}$
FW	954.26
radiation (Å)	0.71073 (Mo Kα)
instrument	Bruker SMART APEX
temperature (K)	293(2)
space group	$Pn\bar{3}$ (No. 201, origin choice 2)
a (Å)	9.2181(2)
V (Å^3)	783.29(5)
Z	4
ρ_{cal} (g/cm^3)	8.092
F_{000}	1627
μ(Mo Kα) (mm^{-1})	71.118
independent reflections [$I > 2\sigma(I)$]	711
R_{int}	0.0419
$R1$; $wR2$; GOF	0.0316; 0.0625; 1.144

A small deficiency at the Cr site was observed. The Bi2 site was found to be a split site around 3-fold axis in $Pn\bar{3}$, but no Bi deficiency was found at the Bi1 and Bi2 sites. In Table 3, we list the selected bond lengths and bond-valence sums (BVS).[24] The BVS values of Bi sites are close to the formal ionic value of +3. Figure 2 gives a picture of the crystal structure of $Bi_3Cr_{2.91}O_{11}$. The composition of $Bi_3Cr_{2.91}O_{11}$ gives (almost) the following charge distribution $Bi^{3+}{}_3Cr^{4+}{}_{1.45}Cr^{5+}{}_{1.45}O_{11}$. Therefore, there is almost a 1:1 mixture of Cr^{4+} and Cr^{5+} ions in this compound.

Magnetic susceptibilities of $Bi_3Cr_{2.91}O_{11}$ showed a small difference between the ZFC and FC curves at 100 Oe and a sharp transition near 220 K (Figure 3). FC susceptibilities were almost temperature-independent and reached saturation below 220 K. This behavior is typical for ferromagnets. The M versus H curves of $Bi_3Cr_{2.91}O_{11}$ at 5 K showed soft ferromagnetic behavior with the saturation of about 4.5 μ_B/f.u. This value is close to the expected value of 4.35 μ_B/f.u. for $Cr^{4+}{}_{1.45}Cr^{5+}{}_{1.45}$. The resistivity of $Bi_3Cr_{2.91}O_{11}$ at RT was too high to be measured with our PPMS system (therefore, it should exceed about 5×10^4 Ω cm). We note that many single crystals were checked, and in all of them, the resistivity was too high to be measured.

In principle, different combinations of Cr^{3+}, Cr^{4+}, Cr^{5+}, and Cr^{6+} can provide electric neutrality in $Bi_3Cr_{2.91}O_{11}$ (see Supporting Information). In $KSbO_3$-type compounds, elements with different oxidation states can occupy the "Sb" site,

Table 3. Selected Bond Distance: (r (Å)) and Bond Valence Sum (BVS)

Bi1−O2 (× 2)	2.340(5)	Bi2−O2	2.179(4)
Bi1−O3 (× 6)	2.461(3)	Bi2−O2	2.208(5)
BVS[a](Bi1)	+3.252	Bi2−O2	2.368(3)
Cr−O1 (× 2)	1.888(3)	Bi2−O1	2.587(4)
Cr−O3 (× 2)	1.914(3)	Bi2−O3	2.626(7)
Cr−O3 (× 2)	1.938(3)	Bi2−O3	2.628(6)
BVS[a](Cr^{6+})	+4.351	Bi2−O1	2.826(5)
BVS[a](Cr^{3+})	+3.601	Bi2−O3	2.855(6)
		Bi2−O1	2.865(6)
		BVS[a](Bi2)	+3.134

[a]BVS = $\sum_{i=1}^{N} v_i$, $v_i = \exp[(r_0 - r_i)/B]$, N is the coordination number, B = 0.37, $r_0(Bi^{3+})$ = 2.094, $r_0(Cr^{3+})$ = 1.724, $r_0(Cr^{6+})$ = 1.794.

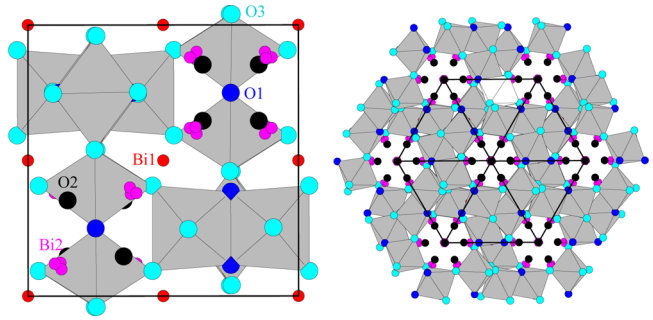

Figure 2. Crystal structure of $Bi_3Cr_{2.91}O_{11}$ viewed along (left) the a axis and (right) the ⟨111⟩ direction. Gray octahedra show CrO_6 units.

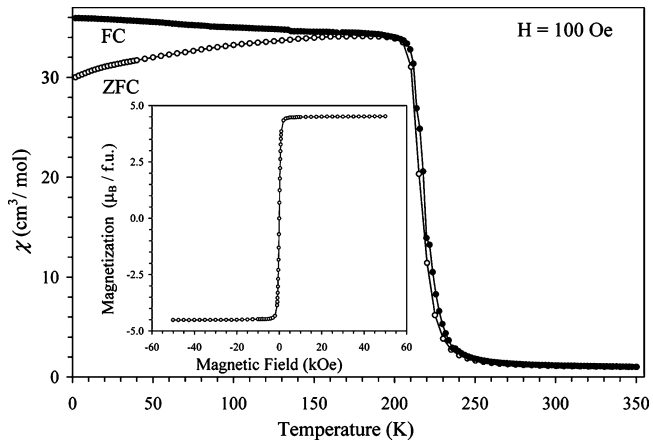

Figure 3. ZFC (○) and FC (●) dc magnetic susceptibility (χ = **M**/**H**) curves of $Bi_3Cr_{2.91}O_{11}$ measured at 100 Oe. (inset) The isothermal magnetization curve at 5 K.

Table 2. Structure Parameters of $Bi_3Cr_{2.91}O_{11}$ at 293 K

site	WP[a]	g[b]	x	y	z	U_{eq} (Å^2)
Bi1	4b	1	0.0	0.0	0.0	0.02136(10)
Bi2	24h	1/3	0.4010(3)	0.3766(5)	0.3802(7)	0.0229(4)
Cr	12g	0.969(6)	0.59598(10)	0.75	0.25	0.0138(2)
O1	12f	1	0.6150(4)	0.25	0.25	0.0152(7)
O2	8e	1	0.1466(3)	x	x	0.0134(7)
O3	24h	1	0.5398(3)	0.2471(3)	0.5929(3)	0.0143(4)

[a]WP = Wyckoff position. [b]g = site occupancy.

dx.doi.org/10.1021/ic500773b | Inorg. Chem. 2014, 53, 8362−8366

$Bi_3(Ga^{3+}Sb_2^{5+})O_{11}$,[25] $(Bi_2Na)Sb^{5+}{}_3O_{11}$,[26] $La_3(Ru_2^{4+}Ru^{5+})O_{11}$,[27] $Bi_3Ge_3^{4+}O_{10.5}$,[28] $Bi_3Mn_3^{4+}O_{10.5}$,[15] $Bi_3(Fe_{1.68}^{3+}Te_{1.32}^{6+})O_{11}$,[29] $Bi_3(Mn_{1.1}^{3+}Mn_{0.8}^{4+}Te_{1.1}^{6+})O_{11}$.[30] For example, Mn^{3+}, Mn^{4+}, and Te^{6+} were found in $Bi_3(Mn_{1.9}Te_{1.1})O_{11}$.[30] Cr^{6+} ions are nonmagnetic, and their presence would perturb magnetic interactions similar to the situation in $Bi_3(Mn_{1.9}Te_{1.1})O_{11}$.[30] Because $Bi_3Cr_{2.91}O_{11}$ shows ferromagnetic ordering at rather high temperature the presence of Cr^{6+} is unlikely. Magnetic measurements cannot distinguish among different combinations of Cr^{3+}, Cr^{4+}, and Cr^{5+} because the saturation magnetization is identical for all combinations, and the effective magnetic moment varies between 4.02 μ_B/f.u. and 4.21 μ_B/f.u., too small for unambiguous conclusions (see Supporting Information). Therefore, we employed the XPS method to get information about oxidation states of Cr (Figure 4).

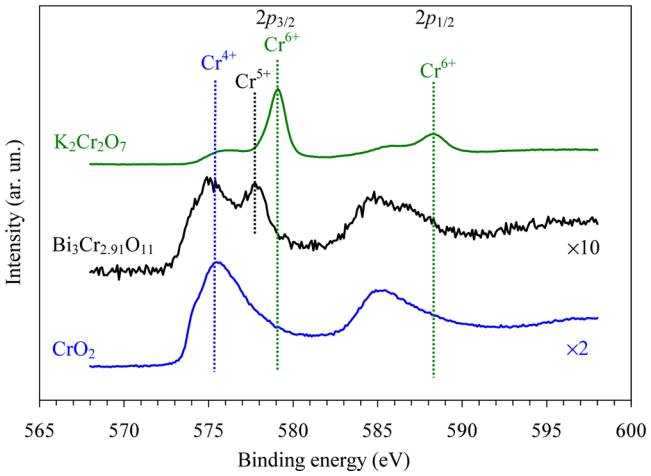

Figure 4. X-ray photoelectron spectra near Cr 2p for $K_2Cr_2O_7$ with Cr^{6+}, $Bi_3Cr_{2.91}O_{11}$, and CrO_2 with Cr^{4+}.

Standard materials with Cr^{6+} (XPS spectra of $CaCrO_4$, $SrCrO_4$, and $BaCrO_4$ were almost identical with that of $K_2Cr_2O_7$, see Supporting Information) showed a sharp peak at 579.0 eV. That peak was absent in $Bi_3Cr_{2.91}O_{11}$ (Figure 4), confirming the absence of Cr^{6+}. The XPS spectrum of $Bi_3Cr_{2.91}O_{11}$ was very close to that of CrO_2, with an additional peak at 577.8 eV. The peak at 577.8 eV could be assigned to Cr^{5+} (we did not have standard materials that would contain only Cr^{5+} ions). Therefore, the XPS measurements confirmed the presence of Cr^{4+} and Cr^{5+}.

We prepared samples with different target compositions, namely, $Bi_3Cr_3O_{11\pm\delta}$, $Bi_{3-\delta}Cr_3O_{11-1.5\delta}$, and $Bi_3Cr_{3-\delta}O_{11-1.5\delta}$. However, the $KSbO_3$-type phases in those samples (without large amounts of impurities) showed very similar lattice parameters (Figure 1), very close magnetic properties (with T_C varying from 205 to 235 K and the saturation magnetization varying from 4.52 μ_B/f.u. to 4.84 μ_B/f.u. (see the Supporting Information)), and almost the same Bi/Cr ratio. These facts confirmed that the chemical composition of the $KSbO_3$-type phases in $Bi_xCr_yO_{11\pm\delta}$ is almost constant (with possible slight variations).

Cr^{4+} and Cr^{5+} ions differ by one electron and statistically occupy one crystallographic site. Therefore, the double-exchange interaction could be one possible origin of ferromagnetism in isostructural $Bi_3Mn_3O_{11.6}$ and $Bi_3Cr_{2.91}O_{11}$ similar, for example, to the $La_{1-x}Sr_xMnO_3$ system with Mn^{3+}/Mn^{4+}. However, double exchange requires large localized core spins, which are absent in $Bi_3Cr_{2.91}O_{11}$ (S = 1/2 for Cr^{5+} and S = 1 for Cr^{4+}). In addition, the double-exchange mechanism usually leads to metallic properties.[31,32] But there are some exceptions; for example, the $La_{1-x}Sr_xMnO_3$ system at small doping levels of $x \approx 0.1$ has small-bandgap semiconducting behavior,[7] and an insulator version of double-exchange ferromagnetism was recently established.[32] Other mechanisms, such as charge ordering proposed for $K_2Cr_8O_{16}$,[31] specific orbital ordering proposed for $BiMnO_3$,[12] and rock-salt ordering of different transition metals observed in R_2NiMnO_6 (R = La–Lu and Y),[2,14] cannot be directly applied for $Bi_3Cr_{2.91}O_{11}$. However, some local charge (Cr^{4+}/Cr^{5+}) or orbital order could give rise to ferromagnetic rather than antiferromagnetic interactions; in this case, a conventional superexchange mechanism could be applicable. Disorder due to the presence of the Cr vacancies could prevent long-range charge or orbital order.

The $KSbO_3$-type structure has a framework built from SbO_6 octahedra and channels filled with potassium atoms. The channels can also accommodate additional oxygen atoms allowing the compositional change from ABO_3 to $ABO_{3.667}$. BO_6 octahedra are connected by an edge forming dimer units. The dimers are connected through corners forming a three-dimensional framework (Figure 2). This framework is different from corner-shared octahedral framework found in perovskites. The presence of mixed-valent 3d transition metals with high oxidation states in the $KSbO_3$-type framework produces ferromagnetism with high T_C and keeps insulating properties as found in $Bi_3Mn_3O_{11.6}$[15] and $Bi_3Cr_{2.91}O_{11}$. Therefore, the $KSbO_3$-type framework is very promising for producing ferromagnetic insulators.

The typical oxidation state of Cr in perovskites is +3, for example, $RCrO_3$ (R = Bi, La–Lu, and Y). With the high-pressure high-temperature method, Cr^{4+} can be stabilized in the octahedral coordination of perovskites, for example, $SrCrO_3$. Cr^{3+}/Cr^{4+} mixed-valent perovskites can also be prepared.[33] Cr^{4+} and Cr^{5+} ions usually have tetrahedral coordination in oxides. Therefore, the presence of the 1:1 mixture of Cr^{4+} and Cr^{5+} in $Bi_3Cr_{2.91}O_{11}$ in octahedral coordination is quite unusual. Mixed-valent chromium compounds are attracting more and more attention because of interesting physical properties.[33,34] An example of $Bi_3Cr_{2.91}O_{11}$ shows that the $KSbO_3$-type structure is quite good for stabilizing transition metals in high oxidation states and in mixed-valent oxidation states.

CONCLUSION

In conclusion, we prepared a new compound, $Bi_3Cr_{2.91}O_{11}$, by the high-pressure high-temperature method. It crystallizes in the $KSbO_3$-type structure. It is a unique compound because (1) it has chromium ions in the unusual oxidation states of Cr^{4+} and Cr^{5+} in octahedral coordination and (2) it exhibits ferromagnetic and, at the same time, insulating properties. The $KSbO_3$-type framework is quite promising for producing ferromagnetic insulators.

ASSOCIATED CONTENT

Supporting Information

Crystallographic information file (cif) of $Bi_3Cr_{2.91}O_{11}$, XRPD patterns and magnetic properties of $Bi_3Cr_{1.5}Mn_{1.5}O_{11}$, $Bi_3Cr_{1.5}Ru_{1.5}O_{11}$, $Bi_3Cr_3O_{11\pm\delta}$, $Bi_{3-\delta}Cr_3O_{11-1.5\delta}$, and $Bi_3Cr_{3-\delta}O_{11-1.5\delta}$; XPS spectra of $CaCrO_4$, $SrCrO_4$, and $BaCrO_4$. This material is available free of charge via the Internet at http://pubs.acs.org.

dx.doi.org/10.1021/ic500773b | Inorg. Chem. 2014, 53, 8362–8366

AUTHOR INFORMATION

Corresponding Author

*E-mail: Alexei.Belik@nims.go.jp.

Notes

The authors declare no competing financial interest.

ACKNOWLEDGMENTS

This work was supported by World Premier International Research Center Initiative (WPI Initiative, MEXT, Japan), the Japan Society for the Promotion of Science (JSPS) through its "Funding Program for World-Leading Innovative R&D on Science and Technology (FIRST Program)", and the Grants-in-Aid for Scientific Research (22246083) from JSPS, Japan. We thank Dr. Hiroya Sakurai of NIMS for providing the $CaCrO_4$, $SrCrO_4$, and $BaCrO_4$ standard materials for the XPS measurements.

REFERENCES

(1) Wolf, S. A.; Awschalom, D. D.; Buhrman, R. A.; Daughton, J. M.; von Molnar, S.; Roukes, M. L.; Chtchelkanova, A. Y.; Treger, D. M. *Science* **2001**, *294*, 1488−1495.

(2) Rogado, N. S.; Li, J.; Sleight, A. W.; Subramanian, M. A. *Adv. Mater.* **2005**, *17*, 2225−2227.

(3) Kittel, C. *Introduction to Solid State Physics;* Wiley: New York, 1996.

(4) Mahadevan, P.; Aryasetiawan, F.; Janotti, A.; Sasaki, T. *Phys. Rev. B* **2009**, *80*, 035106. (b) Lee, S.; Zhang, J. R.; Torii, S.; Choi, S.; Cho, D.-Y.; Kamiyama, T.; Yu, J.; McEwen, K. A.; Park, J.-G. *J. Phys.: Condens. Matter* **2013**, *25*, 465601.

(5) Topfer, J.; Goodenough, J. B. *J. Solid State Chem.* **1997**, *130*, 117−285.

(6) Maurin, I.; Barboux, P.; Lassailly, Y.; Boilot, J. P.; Villain, F.; Dordor, P. *J. Solid State Chem.* **2001**, *160*, 123−133.

(7) Edwards, D. M. *Adv. Phys.* **2002**, *51*, 1259−1318.

(8) Torrance, J. B.; Shafer, M. W.; McGuire, T. R. *Phys. Rev. Lett.* **1972**, *29*, 1168−1171.

(9) Macdonald, H.; Schiffer, P.; Samarth, N. *Nat. Mater.* **2005**, *4*, 195−202.

(10) Matsumoto, Y.; Murakami, M.; Shono, T.; Hasegawa, T.; Fukumura, T.; Kawasaki, M.; Ahmet, P.; Chikyow, T.; Koshihara, S.; Koinuma, H. *Science* **2001**, *291*, 854−856.

(11) Kimura, T.; Kawamoto, S.; Yamada, I.; Azuma, M.; Takano, M.; Tokura, Y. *Phys. Rev. B* **2003**, *67*, 180401.

(12) (a) Moreira dos Santos, A.; Cheetham, A. K.; Atou, T.; Syono, Y.; Yamaguchi, Y.; Ohoyama, K.; Chiba, H.; Rao, C. N. R. *Phys. Rev. B* **2002**, *66*, 064425. (b) Gonchar, L. E.; Nikiforov, A. E. *Phys. Rev. B* **2013**, *88*, 094401.

(13) Hasegawa, K.; Isobe, M.; Yamauchi, T.; Ueda, H.; Yamaura, J.-I.; Gotou, H.; Yagi, T.; Sato, H.; Ueda, Y. *Phys. Rev. Lett.* **2009**, *103*, 146403.

(14) (a) Asai, K.; Fujiyoshi, K.; Nishimori, N.; Satoh, Y.; Kobayashi, Y.; Mizoguchi, M. *J. Phys. Soc. Jpn.* **1998**, *67*, 4218−4228. (b) Booth, R. J.; Fillman, R.; Whitaker, H.; Nag, A.; Tiwari, R. M.; Ramanujachary, K. V.; Gopalakrishnan, J.; Lofland, S. E. *Mater. Res. Bull.* **2009**, *44*, 1559−1564.

(15) Belik, A. A.; Takayama-Muromachi, E. *J. Am. Chem. Soc.* **2010**, *132*, 12426−12432.

(16) Belik, A. A.; Takayama-Muromachi, E. *J. Am. Chem. Soc.* **2009**, *131*, 9504−9505.

(17) Izumi, F.; Ikeda, T. *Mater. Sci. Forum* **2000**, *321*−*324*, 198−203.

(18) *SMART, Molecular analysis research tool;* Bruker AXS Inc.: Madison, WI, 2001.

(19) *SAINT, Data reduction and correction program;* Bruker AXS Inc.: Madison, WI, 2001.

(20) *SADABS, An empirical absorption correction program;* Bruker AXS Inc.: Madison, WI, 2001.

(21) Sheldrick, G. M. *Acta Crystallogr., Sect. A* **2008**, *64*, 112−122.

(22) Farrugia, L. J. *J. Appl. Crystallogr.* **1999**, *32*, 837−838.

(23) Mairesse, G.; Roussel, P.; Vannier, R. N.; Anne, M.; Pirovano, C.; Nowogrocki, G. *Solid State Sci.* **2003**, *5*, 851−859.

(24) Brese, N. E.; O'Keeffe, M. *Acta Crystallogr., Sect. B* **1991**, *47*, 192−197.

(25) (a) Ismunandar; Kennedy, B. J.; Hunter, B. A. *Solid State Commun.* **1998**, *108*, 649−654. (b) Ismunandar; Kennedy, B. J.; Hunter, B. A. *J. Solid State Chem.* **1996**, *127*, 178−185.

(26) Champarnaud-Mesjard, J. C.; Frit, B.; Aftati, A.; El Farissi, M. *Eur. J. Solid State Inorg. Chem.* **1995**, *32*, 495−504.

(27) (a) Cotton, F. A.; Rice, C. E. *J. Solid State Chem.* **1978**, *25*, 137−142. (b) Abraham, F.; Trehoux, J.; Thomas, D. *Mater. Res. Bull.* **1978**, *13*, 805−810. (c) Khalifah, P.; Nelson, K. D.; Jin, R.; Mao, Z. Q.; Liu, Y.; Huang, Q.; Gao, X. P. A.; Ramirez, A. P.; Cava, R. J. *Nature* **2001**, *411*, 669−671. (d) Khalifah, P.; Cava, R. J. *Phys. Rev. B* **2001**, *64*, 085111.

(28) Cheng, J.; Rettie, A. J. E.; Suchomel, M. R.; Zhou, H.; Yan, J.; Song, J.; Marshall, L. G.; Larregola, S. A.; Zhou, J.; Goodenough, J. B. *Inorg. Chem.* **2013**, *52*, 2138−2141.

(29) Valant, M.; Babu, G. S.; Vrcon, M.; Kolodiazhnyi, T.; Axelsson, A.-K. *J. Am. Ceram. Soc.* **2012**, *95*, 644−650.

(30) Li, M.-R.; Retuerto, M.; Bok Go, Y.; Emge, T. J.; Croft, M.; Ignatov, A.; Ramanujachary, K. V.; Dachraoui, W.; Hadermann, J.; Tang, M.-B.; Zhao, J.-T.; Greenblatt, M. *J. Solid State Chem.* **2013**, *197*, 543−549.

(31) Mahadevan, P.; Kumar, A.; Choudhury, D.; Sarma, D. D. *Phys. Rev. Lett.* **2010**, *104*, 256401.

(32) Nishimoto, S.; Ohta, Y. *Phys. Rev. Lett.* **2012**, *109*, 076401.

(33) Arevalo-Lopez, A. M.; Rodgers, J. A.; Senn, M. S.; Sher, F.; Farnham, J.; Gibbs, W.; Attfield, J. P. *Angew. Chem., Int. Ed.* **2012**, *51*, 10791−10794.

(34) Sakurai, H.; Kolodiazhnyi, T.; Michiue, Y.; Takayama-Muromachi, E.; Tanabe, Y.; Kikuchi, H. *Angew. Chem., Int. Ed.* **2012**, *51*, 6653−6656.